

Neuroigin-4 is localized to glycinergic postsynapses and regulates inhibition in the retina

Mrinalini Hoon^{a,b,1}, Tolga Soykan^{a,2}, Björn Falkenburger^{b,c,2,3}, Matthieu Hammer^{a,b}, Annarita Patrizi^d, Karl-Friedrich Schmidt^e, Marco Sassoè-Pognetto^d, Siegrid Löwel^{e,4}, Tobias Moser^{b,f}, Holger Taschenberger^g, Nils Brose^{a,b,5}, and Frédérique Varoqueaux^{a,b,5}

^aDepartment of Molecular Neurobiology, Max Planck Institute of Experimental Medicine, D-37075 Göttingen, Germany; ^bDeutsche Forschungsgemeinschaft Research Center for Molecular Physiology of the Brain, D-37075 Göttingen, Germany; ^cDepartment of Neurodegeneration and Restorative Research, University of Göttingen, D-37075 Göttingen, Germany; ^dDepartment of Anatomy, Pharmacology, and Forensic Medicine, and National Institute of Neuroscience, I-10126 Turin, Italy; ^eInstitute of General Zoology and Animal Physiology, Friedrich Schiller University, D-07743 Jena, Germany; ^fDepartment of Otolaryngology, University of Göttingen, D-37075 Göttingen, Germany; and ^gDepartment of Membrane Biophysics, Max Planck Institute of Biophysical Chemistry, D-37077 Göttingen, Germany

Edited by Thomas C. Südhof, Stanford University School of Medicine, Palo Alto, CA, and approved January 12, 2011 (received for review May 25, 2010)

Neuroigins (NL1–NL4) are postsynaptic adhesion proteins that control the maturation and function of synapses in the central nervous system (CNS). Loss-of-function mutations in NL4 are linked to rare forms of monogenic heritable autism, but its localization and function are unknown. Using the retina as a model system, we show that NL4 is preferentially localized to glycinergic postsynapses and that the loss of NL4 is accompanied by a reduced number of glycine receptors mediating fast glycinergic transmission. Accordingly, NL4-deficient ganglion cells exhibit slower glycinergic miniature postsynaptic currents and subtle alterations in their stimulus-coding efficacy, and inhibition within the NL4-deficient retinal network is altered as assessed by electroretinogram recordings. These data indicate that NL4 shapes network activity and information processing in the retina by modulating glycinergic inhibition. Importantly, NL4 is also targeted to inhibitory synapses in other areas of the CNS, such as the thalamus, colliculi, brainstem, and spinal cord, and forms complexes with the inhibitory postsynapse proteins gephyrin and collybistin *in vivo*, indicating that NL4 is an important component of glycinergic postsynapses.

synaptogenesis | inhibitory transmission | visual processing

In rodents, postsynaptic adhesion proteins of the neuroigin family (NL1–NL4) are expressed throughout the central nervous system (CNS) (1–3) and essential for synapse organization and function (2–5). *In vivo*, each NL isoform localizes to specific synapse subpopulations, with NL1, NL2, and NL3 predominantly associating with glutamatergic, GABAergic, or both types of postsynapses, respectively (1, 6–9).

Thus far, the distribution and function of the fourth NL isoform has remained unclear, despite the wide interest triggered by the causal link of specific loss-of-function mutations in NL4 to cases of autism, which led to the notion that aberrant synaptic transmission may cause autism spectrum disorders (ASDs) (10).

We examined the distribution of NL4 in the mouse retina, a well-characterized region of the CNS with distinct, topographically organized glutamatergic, GABAergic, and glycinergic synapses, which has recently allowed us to characterize crucial aspects of NL2 distribution and function (8). Additionally, we assessed NL4 function by studying synaptic activity and visual processing in the NL4-deficient (NL4-KO; ref. 3) mouse retina. Finally, we studied NL4 localization in the rest of the CNS and identified some of its key binding partners at the synapse.

Results

NL4 Is Localized to Glycinergic Postsynapses in the Retina. We characterized the distribution of NL4 by immunohistochemistry by using an isoform-specific antibody (3) (Fig. 1). A punctate labeling was detected in the inner plexiform layer (IPL) of wild-type (WT) but not NL4-KO retinae (Fig. 1A). NL4-positive puncta were abundant in the outer IPL but sparse in the rest of the IPL (Fig. 1A), which is reminiscent of glycine receptor

(GlyR) distribution in the retina (11, 12). Indeed, upon colabeling with a pan-GlyR antibody (mAb4a; ref. 13), the majority of NL4 puncta overlapped with GlyR clusters ($73.5 \pm 4.2\%$, $n = 5$ mice; Fig. 1B, *Left*), whereas only a small fraction colocalized with GABA_A receptors labeled for the ubiquitous $\gamma 2$ subunit ($18.4 \pm 6\%$, $n = 5$ mice). NL4 puncta were absent from excitatory postsynaptic specializations, as judged by colabeling for the excitatory postsynapse marker PSD-95 ($1.9 \pm 0.8\%$, $n = 5$ mice; Fig. 1B, *Right*). Thus, NL4 is localized to inhibitory, preferentially glycinergic synapses in the retina and is the only NL isoform to display such selectivity.

Glycinergic transmission is essential for visual transmission. GlyR-bearing synapses are present on bipolar cell terminals, amacrine cell processes, and retinal ganglion cell (RGC) dendrites (12) and control the efficient coding of information by RGCs, the output cells of the retina. We therefore determined the fraction of glycinergic postsynapses that contain NL4 and found that NL4 equips a subset of glycinergic synapses in the retina ($21.3 \pm 3.5\%$, $n = 5$ mice). Thus, a deficiency of NL4 might lead to altered visual processing and information transfer in the IPL.

Loss of NL4 Causes a Reduction in GlyR Number and Slower Glycinergic mIPSCs. To investigate retinal structure and function in the absence of NL4, we carried out immunolabelings for diverse cellular and synaptic markers (Fig. S1; $n = 8$ pairs), which demonstrated that the main excitatory pathway and the GABAergic circuitry are not altered in NL4-KO retina. These results indicate that NL4 loss does not detectably affect the overall formation of the retinal circuitry. Expression levels of NL1–3 were unchanged in NL4-KO retina homogenates compared with WT (Fig. S2A), and the number of clusters immunoreactive for NL2, the other NL isoform present at inhibitory retinal synapses (8), was similar in WT and NL4-KO (Fig. S2B and C), indicating that the lack of NL4 is not detectably compensated by an up-regulation of NL1–3 expression.

Author contributions: M. Hoon, B.F., N.B., and F.V. designed research; M. Hoon, T.S., B.F., M. Hammer, A.P., K.-F.S., and M.S.-P. performed research; M. Hoon, B.F., K.-F.S., S.L., T.M., H.T., and F.V. analyzed data; and M. Hoon, B.F., N.B., and F.V. wrote the paper.

The authors declare no conflict of interest.

This article is a PNAS Direct Submission.

¹Present address: Department of Biological Structure, University of Washington, Seattle, WA 98195.

²T.S. and B.F. contributed equally to this work.

³Present address: Department of Physiology and Biophysics, University of Washington, Seattle, WA 98195.

⁴Present address: School of Biology and Bernstein Focus for Neurotechnology, University of Göttingen, D-37077 Göttingen, Germany.

⁵To whom correspondence may be addressed. E-mail: varoqueaux@em.mpg.de or brose@em.mpg.de.

This article contains supporting information online at www.pnas.org/lookup/suppl/doi:10.1073/pnas.1006946108/-DCSupplemental.

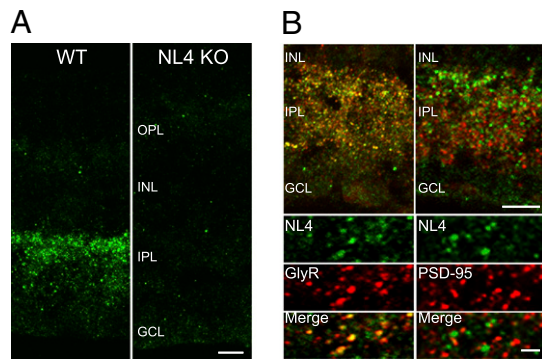


Fig. 1. NL4 associates with GlyRs. In the retina, NL4 staining yielded a robust, punctate labeling in WT but not in NL4-KO mice (A). In the IPL, NL4 clusters colocalized extensively with GlyRs (B Left) but not with PSD-95 (B Right). OPL, outer plexiform layer; INL, inner nuclear layer; IPL, inner plexiform layer; GCL, ganglion cell layer. (Scale bars: A and B Upper, 10 μm ; B Lower, 1 μm).

To assess the integrity of glycinergic postsynapses, immunolabeling was performed for physiologically distinct populations of GlyRs, labeled with antibodies against $\alpha 1$ – $\alpha 4$ subunits (12). There was no obvious alteration in overall GlyR cluster distribution or density in the NL4-KO (Fig. 2A). Upon quantification, however, a significant reduction in the number of GlyR $\alpha 1$ clusters was detected in NL4-KO retinæ (Fig. 2B; WT_{mean}, 19.08 \pm 0.77 puncta per 100 μm^2 of IPL; KO_{mean}, 15.88 \pm 0.59 puncta per 100 μm^2 of IPL, $n = 7$ pairs, $P = 0.006$).

To test whether this reduction in GlyR $\alpha 1$ clusters is functionally relevant, we performed whole-cell patch-clamp recordings from RGCs in a whole-mount preparation to preserve synaptic connectivity of RGCs. A combination of morphological and functional criteria was used to ensure that recordings exclusively originated from RGCs. We recorded miniature inhibitory postsynaptic currents (mIPSCs) from WT and NL4-KO cells in the presence of NBQX, AP5, and bicuculline to pharmacologically isolate glycinergic events. Approximately one-third of RGCs exhibited glycinergic mIPSCs (WT, $n = 13$ mice, 25 cells; KO, $n = 10$ mice, 16 cells). Both ON- and OFF-type RGCs displayed glycinergic mIPSCs, independently of the genotype. Moreover, the frequency of these events was similar in WT and NL4-KO cells (Fig. 2D, $P = 0.613$), reflecting the integrity of glycinergic innervation despite the lack of NL4.

Average glycinergic mIPSC amplitudes were not significantly smaller in NL4-KO RGCs compared with WT cells (Fig. 2C and D; WT_{mean}, 27.40 \pm 2.25 pA; KO_{mean}, 22.98 \pm 2.44 pA; $P = 0.192$). Kinetic analysis revealed that the time-to-peak (20–80%; Fig. 2D) of glycinergic mIPSCs from NL4-KO RGCs was not significantly longer (WT_{mean}, 316 \pm 8 μs ; KO_{mean}, 362 \pm 23 μs ; $P = 0.079$). However, their average decay time constant (τ) was significantly longer compared with WT RGCs (Fig. 2C and D; τ_{WT} , 2.42 \pm 0.10 ms; τ_{KO} , 2.87 \pm 0.15 ms; $P = 0.022$). Correspondingly, the cumulative distribution function generated from τ values of individual events showed a shift toward longer values for the NL4-KO (Fig. 2E; WT_{mean}, 2.50 \pm 0.04 ms; KO_{mean}, 2.68 \pm 0.05 ms, $P = 0.022$). Above data show that some of the fastest glycinergic events are absent in NL4-KO RGCs. Because GlyR $\alpha 1$ is known to confer fast kinetics to GlyRs (14), these results are consistent with the selective reduction in GlyR $\alpha 1$ clusters observed morphologically (Fig. 2B).

To verify the specificity of these findings, we recorded GABAergic mIPSCs from RGCs in the presence of NBQX, AP5, and strychnine (WT: $n = 7$ animals, 20 cells; KO: $n = 7$ animals, 22 cells). None of the tested parameters of GABAergic mIPSCs was altered in NL4-KO cells (Fig. 2F; $P > 0.3$), demonstrating that glycinergic inputs to RGCs are specifically impaired in the NL4-KO.

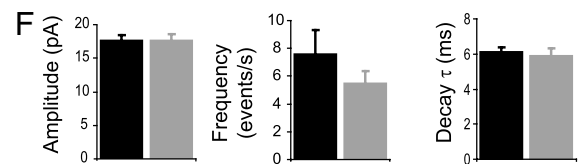
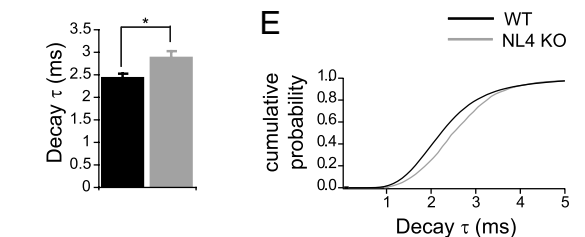
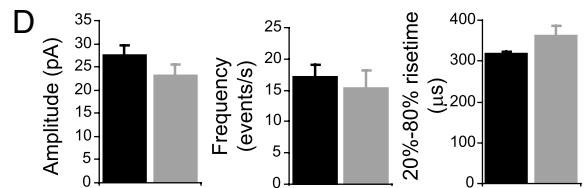
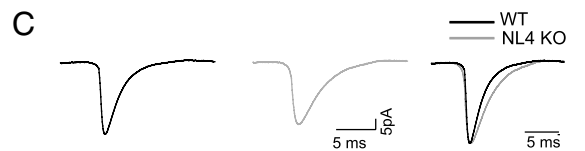
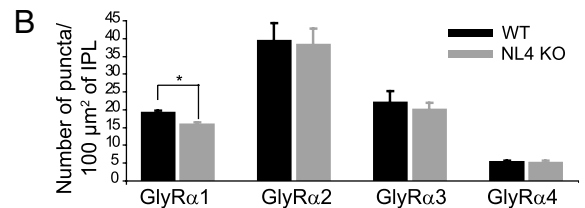
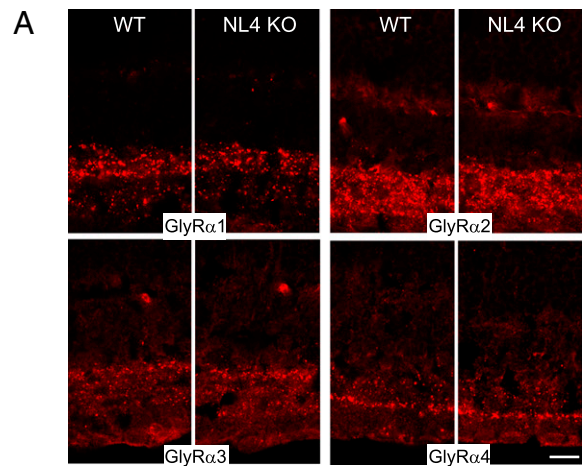


Fig. 2. NL4 loss causes alterations of the glycinergic circuit. Distinct populations of GlyRs bearing $\alpha 1$ – $\alpha 4$ subunits were similarly distributed in WT and NL4-KO retinæ (A). Quantitative analysis uncovered a specific reduction in the number of GlyR $\alpha 1$ clusters in NL4-KO retinæ (B). Glycinergic (C–E) and GABAergic (F) mIPSCs were recorded from WT and NL4-KO RGCs. (C) Example traces of WT and NL4-KO glycinergic mIPSCs. (D) Glycinergic mIPSCs from NL4-KO RGCs were not significantly different in frequency, amplitude, and rise time, but showed significantly slower decay kinetics compared with WT. Cumulative histogram of decay time constant (τ) values of glycinergic mIPSCs (E) showed a rightward shift in the KO. Amplitude, frequency, and decay time constant (τ) of GABAergic mIPSCs were similar in WT and NL4-KO RGCs. (Scale bar: 5 μm .)

0.001). Similarly, contrast sensitivity (measured at six different spatial frequencies) was unaltered in NL4-KOs (Fig. 3E), but significantly reduced in NL2-KOs (Fig. 3F). This reduction was largest at the optimal spatial frequency to which the inhibitory system is tuned (0.064 cycle per degree; Fig. 3F). Thus, loss of NL2 is more detrimental to visual processing than NL4 loss. Together, above data show that different NL isoforms contribute differentially to visual information processing, and that NL4 loss has an effect on visual processing in the retina but does not detectably affect visual acuity and contrast sensitivity.

NL4 Is Present at Inhibitory Synapses Throughout the CNS. To test whether the association of NL4 with glycinergic synapses is a general feature, we analyzed its distribution in the rest of the CNS. We found NL4 to be expressed throughout the brain (Fig. 4 and Figs. S4 and S5), in agreement with a previous study (3). Interestingly, NL4 immunoreactivity was faint or diffuse in many forebrain areas (Fig. 4 and Figs. S4 and S5), such as the olfactory bulb, the cortex (strongest in layer IV; Fig. 4A and Fig. S5A), and the hippocampus (Fig. S5A), and did not correlate with synaptic markers, yet it was clustered in most other regions, e.g., in basal ganglia (globus pallidus; Fig. 4C), midbrain (colliculi; Fig. 4C), and thalamus (Fig. 4C). In the latter regions, NL4 labeling was intense and punctate, and colocalized preferentially with the inhibitory synapse scaffold protein gephyrin, but not with the excitatory synapse scaffold protein PSD-95 (Fig. 4C and Figs. S4 and S5B). NL4 labeling was particularly robust in brainstem (Fig. 4A and C) and spinal cord (Fig. 4B and C), where glycinergic neurotransmission is prominent (20, 21). In these regions, the vast majority of NL4 immunoreactive puncta were associated with GlyR-positive clusters and not with PSD-95 (Fig. 4C). These findings correlate with our observations in the retina (Fig. 1), implying that NL4 associates prominently with inhibitory (glycinergic) postsynapses throughout the CNS.

NL4 Binds Gephyrin and Collybistin. The scaffolding protein gephyrin is essential for GlyR clustering in retina and brainstem (22, 23), and all NLS bind gephyrin via a conserved cytoplasmic motif (24). However, so far only NL2 is known to selectively induce gephyrin clustering at inhibitory postsynapses by simultaneously binding to the gephyrin-binding protein collybistin (CB2^{SH3+}; ref. 24 and Fig. 5B). We found that the intracytoplasmic domain of NL4 (NL4_{ICD}) also interacts with gephyrin and collybistin in yeast two-hybrid assays (Fig. 5A) and GST-pulldowns (Fig. 5B). In contrast, NL1_{ICD} and NL3_{ICD} bind only gephyrin (24) but not collybistin (ref. 24 and Fig. 5B). Further, NL4_{ICD} induces the formation of NL, gephyrin, and collybistin submembranous microaggregates in heterologous cells (Fig. 5C and Fig. S6), as does NL2_{ICD} (24). Finally, gephyrin and collybistin are coimmunoprecipitated with NL4 in chemically cross-linked extracts from mixed brainstem and spinal cord samples of WT and NL2-KO, but not of NL4-KO mice (Fig. 5D), indicating that NL4, gephyrin, and collybistin specifically associate into higher-order complexes *in vivo*.

Interestingly, in the retina we observed that the number of NL4-immunoreactive clusters is significantly up-regulated in the NL2-KO compared with WT (Fig. 5E; WT, 26.00 ± 4.80 NL4 puncta per $100 \mu\text{m}^2$; NL2 KO, 72.51 ± 5.14 NL4 puncta per $100 \mu\text{m}^2$; $n = 7$ pairs; $P < 0.0001$). The NL4 clusters in the NL2-KO retain their specific association with GlyRs and GABA_A receptors ($73 \pm 3\%$ and $18 \pm 4\%$, respectively). However, the proportion of GlyR- (WT, $18 \pm 3\%$; NL2-KO, $44 \pm 6\%$; $n = 3$ pairs; $P = 0.0106$) and GABA_Aγ2-positive puncta (WT, $0.71 \pm 0.2\%$; NL2-KO, $3.18 \pm 0.4\%$; $n = 3$ pairs; $P = 0.0006$) that associate with NL4 is significantly increased in the NL2-KO. Because the majority of NL2 colocalizes with GABA_Aγ2, whereas a subset ($\approx 20\%$) associates with GlyRs (8), our data indicate that NL4 might replace lost NL2 at a subset of postsynapses while retaining its preference for glycinergic synapses. Alternatively, as the number of GlyR postsynapses remains unchanged in the

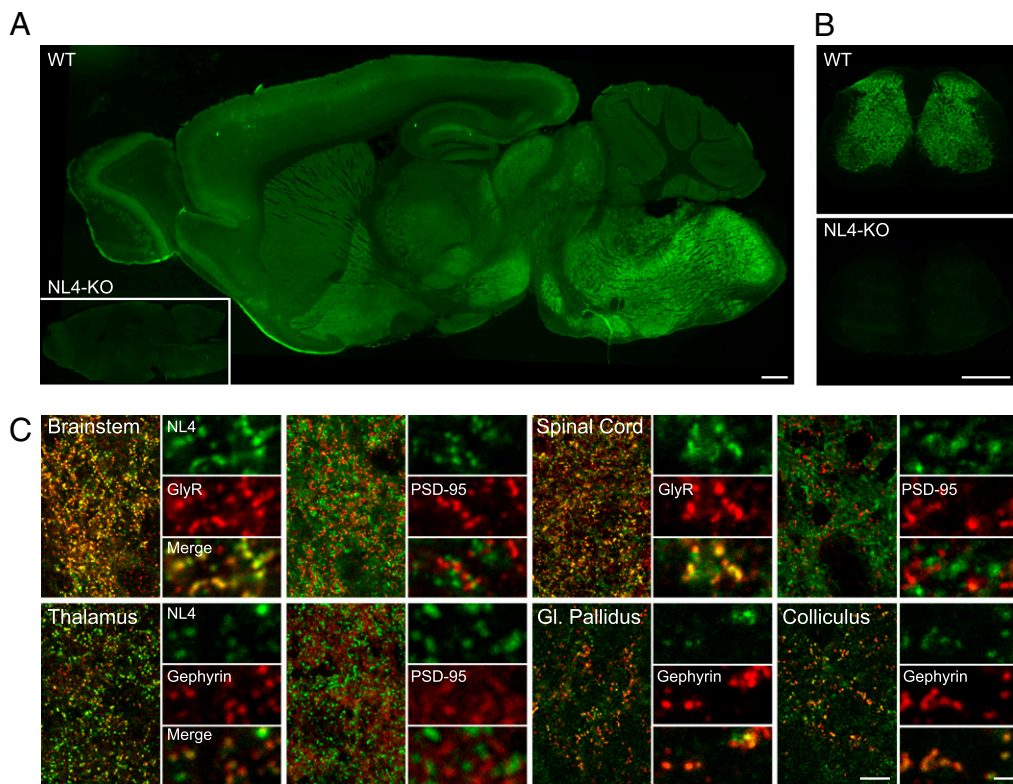


Fig. 4. NL4 distribution in the CNS. NL4 is widely expressed in the brain (A and C), brainstem (A and C) and spinal cord (B and C). NL4 labeling is specific in both brain and spinal cord sections, because no residual staining is left in the NL4-KO (A and B). As exemplified in the cuneate nucleus of the brainstem (C Upper Left) and in the dorsal horn of the spinal cord (C Upper Right), NL4 clusters are located at glycinergic but not glutamatergic postsynapses, as illustrated by a colabeling with GlyRs but not with PSD-95. In the parafascicular thalamic nucleus, NL4 immunoreactive clusters associate specifically with the inhibitory postsynaptic protein gephyrin and do not correlate with PSD-95 puncta (C Lower Left). Similarly in the globus (Gl.) pallidus and superior colliculus, NL4 immunoreactive clusters are specifically localized at gephyrin-immunopositive inhibitory postsynapses (C Lower Right). (Scale bars: A and B, 500 μm ; C, 10 μm ; C detail, 1 μm).

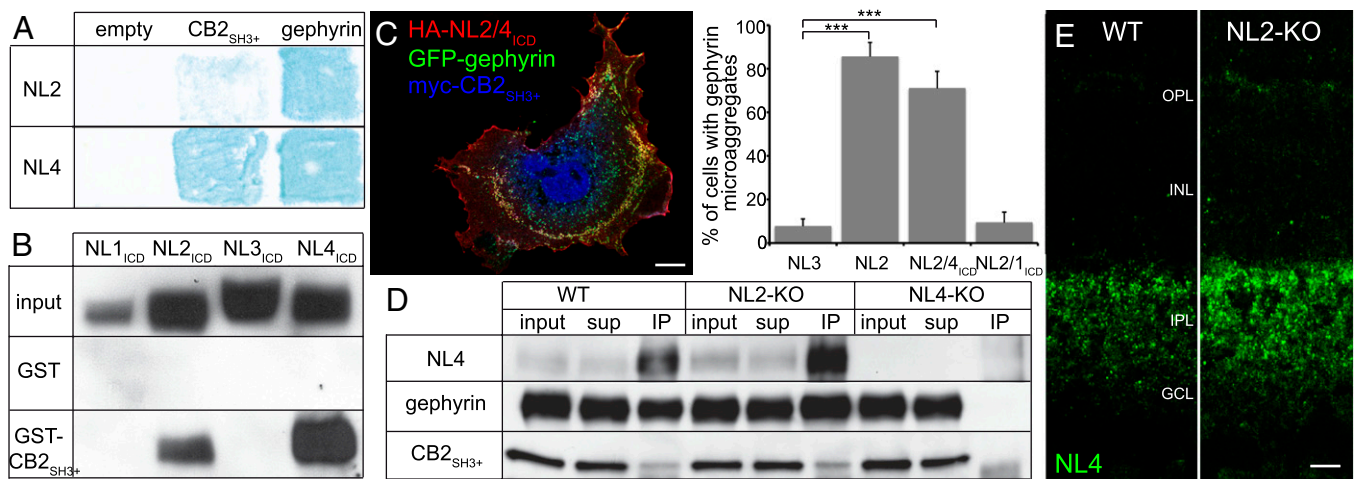


Fig. 5. NL4 interacts with collybistin and gephyrin. The intracytoplasmic domain of NL4 (NL4_{ICD}) binds gephyrin and collybistin (CB2_{SH3+}) in yeast two-hybrid (A) and GST-pulldown assays (B). This feature of NL4 is shared by NL2 but not by NL1 or NL3 (B). Coexpression of GFP-gephyrin, myc-CB2_{SH3+}, and a HA-NL2_{ECD}-NL4_{ICD} (NL2/4_{ICD}) fusion protein in COS7 cells yields to the formation of NL/gephyrin/collybistin microclusters at the plasma membrane (C Left) as NL2 does (C Right). In contrast, HA-NL3 or a HA-NL2_{ECD}-NL1_{ICD} (NL2/1_{ICD}) fusion protein does not produce microaggregates (C Right). Further, gephyrin and collybistin are coimmunoprecipitated with endogenous NL4 from cross-linked homogenates from WT and NL2-KO, but not from NL4-KO (D), showing that these proteins form complexes in vivo. Note that a nonspecific cross-reactive band of unknown nature that runs below the specific collybistin band is detected in all immunoprecipitates. In the NL2-KO retina, the number of NL4-immunoreactive clusters is increased compared with WT (E). (Scale bars: C, 20 μ m; E, 10 μ m.)

NL2-KO (8), NL4 up-regulation might reflect complex network effects in the NL2-KO.

Discussion

NLs are essential for synapse maturation and function (2, 25, 26). NL4 has attracted particular attention because several NL4 loss-of-function mutations were found in patients with ASDs (27–29), and NL4-KO mice show ASD-related behavioral features (3). We show here that NL4 is consistently localized to glycinergic postsynapses (Figs. 1 and 4), and modulates synaptic function (Fig. 2) and network activity in the retina (Fig. 3). Although we focused our analysis on the functional consequences of NL4 deficiency in the adult retina, it is likely that the observed changes upon NL4 loss are the result of developmental effects, e.g., in synapse formation and maturation during late phases of development.

Loss of NL4 is accompanied by a reduction in GlyR α 1 cluster number in the IPL (Fig. 2B). This decrease is the likely cause of the slower kinetics of glycinergic mIPSCs in NL4-KO RGCs (Fig. 2 C–E), as complete loss of GlyR α 1 clusters causes a twofold increase in decay time constants of glycinergic IPSCs (14). Prolonged glycinergic currents may result in impaired inhibition or mitigate excitatory inputs from bipolar cells, either way affecting RGC output. Indeed, upon application of a robust visual stimulus (white noise), the output of NL4-KO RGCs was altered. Mutant cells apportioned a larger fraction of spikes to code for light in comparison with WT cells, and displayed reduced response latency, in line with an impaired inhibition (Fig. 3B).

Interestingly, NL4 loss also affects visual processing upstream of RGCs, as indicated by the reduced amplitude of the ERG b-wave (Fig. 3D), which reflects bipolar cell activity. It is classically attributed to activity at bipolar cell dendrites but also influenced by synaptic input and electrical coupling onto bipolar cell axons in the IPL (30). Since NL4 is only present in the IPL, and since GlyRs (in particular those containing the α 1 subunit) provide a robust inhibition onto rod bipolar cells (12), we propose that the reduction of b-wave amplitudes in NL4-KOs reflects alterations in the glycinergic innervation of bipolar cell axons. The oscillatory potentials of the ERG (Fig. 3D), which represent inhibitory feedback loops in the IPL that involve bipolar, amacrine, and RGC processes (31), showed a tendency toward smaller amplitudes in NL4-KOs. This trend would be compatible with a slight alter-

ation in inhibitory processing due to functional changes in a subset of glycinergic synapses in the NL4-KO retina.

NL4-KO mice serve as a model of certain monogenic heritable ASDs (3). We show here that NL4 is selectively associated with glycinergic postsynapses throughout the CNS (Figs. 1 and 4). Interestingly, NL4 immunoreactivity is faint or diffuse in brain regions classically referred to in the context of ASDs (e.g., cortex and hippocampus) (Figs. S4 and S5). In these regions, glycinergic transmission is known to operate via synaptic or extrasynaptic GlyRs (32), and it will be crucial to find out whether NL4 associates with GlyRs in these regions. At any rate, the functional characterization of NL4 in the retina revealed a specific deficit in fast glycinergic transmission in NL4-KOs (Fig. 2 C–E), which is in line with the concept that ASDs may correlate with an increased excitation vs. inhibition ratio (33). Alterations in visual processes [reduced b-wave amplitudes (34); see also ref. 35] have been observed in subsets of ASD patients. In NL4-KOs, we detected reduced ERG b-wave amplitudes (Fig. 3D) in line with these observations, although other measures of visual processing like acuity and contrast sensitivity remained unaltered (Fig. 3E). However, in the NL2-KO mouse, where a pronounced GABAergic deficit is observed both morphologically and functionally (8), visual acuity and contrast sensitivity were dramatically impaired (Fig. 3F).

It will be interesting to see in future studies the relative contributions of glycinergic vs. GABAergic transmission in the determination of acuity and contrast sensitivity. Glycinergic signaling in the retina may be more relevant for features of visual processing that were not captured by our behavioral paradigms. Indeed, processing of contrast and spatial frequency may rely preferentially on the GABAergic system (17, 19). In addition, retinal deficits in the NL4-KO may have been compensated at higher visual centers, which rely more on GABAergic rather than glycinergic interneurons (36, 37).

NL4, like all other NLs, contains a PDZ-binding domain (24, 38) as well as a gephyrin-binding motif (24) and can therefore, in principle, associate with both excitatory and inhibitory postsynaptic scaffolds. We show here that NL4, but not NL1 or NL3, shares with NL2 the ability of binding collybistin, a feature likely related to their specific role at inhibitory postsynapses (ref. 24 and Fig. 5). Moreover, the increased number of NL4 clusters observed in the NL2-KO indicates that NL4 can replace NL2 at a subset of

synapses that would otherwise contain NL2 alone or in combination with NL4, and that NL2 and NL4 are functionally related.

Materials and Methods

Immunohistochemistry. For immunohistochemical analysis, 8- to 10-wk-old animals were used. Retinae were fixed with 2% paraformaldehyde, cryoprotected, and frozen. Fourteen-micrometer vertical sections were collected on slides for immunostaining. Brain, brainstem, and spinal cord were dissected and frozen in isopentane (-35°C). Twenty-micrometer sections were collected on slides and fixed by immersion in methanol (-20°C) for immunostaining. Images were obtained with a TCS-SP2 confocal microscope (Leica Microsystems) and analyzed with AnalySIS (Olympus).

Patch-Clamp Recordings. Whole-cell patch-clamp recordings from RGCs were performed on whole-mount retinae from 3-wk-old mice at room temperature under dim-light conditions. Retinae were dissected in a low- Ca^{2+} artificial CSF (aCSF). Glycinergic or GABAergic mIPSCs were recorded at -70 mV in the presence of TTX, NBQX ($1\ \mu\text{M}$), AP5 ($50\ \mu\text{M}$), and bicuculline ($50\ \mu\text{M}$) or strychnine ($500\ \text{nM}$). The intracellular pipette solution contained $55\ \text{mM}$ Cs-Gluconate, $55\ \text{mM}$ CsCl₂, $1\ \text{mM}$ CaCl₂, $10\ \text{mM}$ EGTA, $10\ \text{mM}$ Na-Hepes, $4\ \text{mM}$ Mg-ATP, $0.4\ \text{mM}$ Na-GTP, $0.1\ \text{mM}$ Alexa 488 (Molecular Probes) at pH 7.3. RGCs were distinguished from displaced amacrine cells by size (diameter $> 15\ \mu\text{m}$), physiology (voltage-activated sodium currents $> 2\ \text{nA}$), and morphology (presence of an axon). Data were analyzed with IGOR Pro-6.1 (Wavemetrics). mIPSCs were detected by using a sliding template algorithm (39).

MEA Recordings. Recordings were performed by using 200/30 MEAs (60 electrodes, $30\ \mu\text{m}$ diameter, $200\ \mu\text{m}$ spacing, 8×8 grid) in oxygenated aCSF at 37°C (8). Large retina pieces were placed with the RGC layer facing the MEA, and light stimuli (1 s ON/2 s OFF stimulus or 10-s-long pseudorandom white noise stimulus) were delivered 200 times by a green light emitting diode (LED) placed at the camera port of an inverted microscope (BX-51; Olympus). Data were analyzed with IGOR Pro-5.03 (Wavemetrics).

In Vivo Vision Assays. Visual acuity and contrast sensitivity were assessed with a virtual-reality optomotor system (40). Scotopic ERGs were recorded by using dark-adapted anesthetized mice and light flashes of incremental calibrated (0.0002 – $14\ \text{cd}\cdot\text{s}/\text{m}^2$) intensities. A full-field illumination (25 white LEDs) was used to produce light flashes, and a moistened AgCl electrode was placed on the cornea to record responses.

Biochemistry. Yeast two-hybrid assays were performed as described (24). For pulldown assays, glutathione-Sepharose beads with GST alone or GST-CB₂SH₃ were incubated with NL_{ICD}-Fc constructs. Bound NL_{ICD}-Fc was analyzed by SDS/PAGE and Western blotting. Coimmunoprecipitation assays were performed on DSP-crosslinked homogenates of brainstem and spinal cord as described (24) from WT, NL2-KO, or NL4-KO, using isoform-specific polyclonal antibodies against NL2 and NL4. Coclustering experiments in COS cells were performed as described by using available HA-NL2, HA-NL3 (24), and newly generated HA-tagged chimeric NL2_{ECD}-NL4_{ICD} and NL2_{ECD}-NL1_{ICD} expression constructs, which encode the NL2 extracellular domain (ECD) fused to the NL4 or NL1 transmembrane and intracellular domains (ICD). The latter constructs were used to compare NL4_{ICD} and NL1_{ICD} as their use circumvents the problem that full-length WT NL4 is not properly trafficked to COS cell plasma membranes.

Further Experimental Details. Statistical comparison of genotypes was carried out by using two-tailed unpaired (Welch corrected) *t* test. Detailed experimental methods are provided in *SI Materials and Methods*.

ACKNOWLEDGMENTS. We thank J. Ammermüller, K. Dedek, J.-M. Fritschy, T. Gollisch, M. Van Wyk, H. Wässle, and R. Wong for helpful discussions and B. Cooper, C. Rüdiger and K. Hellmann for technical support. This work was funded by the Cure Autism Now Foundation (F.V.); the Hertie Foundation (M. Hoon); European Community Grants NEUREST MEST-CT-2004-504193 (to M. Hoon) and EUROSIN-HEALTH-F2-2009-241498 (to N.B.); the Deutsche Forschungsgemeinschaft Center for Molecular Physiology of the Brain (M. Hoon, B.F., M. Hammer, T.M., N.B., and F.V.); a Human Frontier Science Program grant (to S.L.); a Human Frontier Science Program fellowship (to B.F.); and the Max Planck Society (Tandem Project) (N.B. and T.M.).

- Varoqueaux F, Jamain S, Brose N (2004) Neuroligin 2 is exclusively localized to inhibitory synapses. *Eur J Cell Biol* 83:449–456.
- Varoqueaux F, et al. (2006) Neuroligins determine synapse maturation and function. *Neuron* 51:741–754.
- Jamain S, et al. (2008) Reduced social interaction and ultrasonic communication in a mouse model of monogenic heritable autism. *Proc Natl Acad Sci USA* 105:1710–1715.
- Ichtchenko K, et al. (1995) Neuroligin 1: A splice site-specific ligand for beta-neurexins. *Cell* 81:435–443.
- Ichtchenko K, Nguyen T, Südhof TC (1996) Structures, alternative splicing, and neurexin binding of multiple neuroligins. *J Biol Chem* 271:2676–2682.
- Chubykin AA, et al. (2007) Activity-dependent validation of excitatory versus inhibitory synapses by neuroligin-1 versus neuroligin-2. *Neuron* 54:919–931.
- Song JY, Ichtchenko K, Südhof TC, Brose N (1999) Neuroligin 1 is a postsynaptic cell-adhesion molecule of excitatory synapses. *Proc Natl Acad Sci USA* 96:1100–1105.
- Hoon M, et al. (2009) Neuroligin 2 controls the maturation of GABAergic synapses and information processing in the retina. *J Neurosci* 29:8039–8050.
- Budreck EC, Scheiffele P (2007) Neuroligin-3 is a neuronal adhesion protein at GABAergic and glutamatergic synapses. *Eur J Neurosci* 26:1738–1748.
- Bourgeron T (2009) A synaptic trek to autism. *Curr Opin Neurobiol* 19:231–234.
- Wässle H, Koulen P, Brandstätter JH, Fletcher EL, Becker CM (1998) Glycine and GABA receptors in the mammalian retina. *Vision Res* 38:1411–1430.
- Wässle H, et al. (2009) Glycinergic transmission in the mammalian retina. *Front Mol Neurosci* 2:6.
- Kirsch J, Betz H (1993) Widespread expression of gephyrin, a putative glycine receptor-tubulin linker protein, in rat brain. *Brain Res* 621:301–310.
- Majumdar S, Heinze L, Haverkamp S, Ivanova E, Wässle H (2007) Glycine receptors of A-type ganglion cells of the mouse retina. *Vis Neurosci* 24:471–487.
- Fairhall AL, et al. (2006) Selectivity for multiple stimulus features in retinal ganglion cells. *J Neurophysiol* 96:2724–2738.
- Chichilnisky EJ (2001) A simple white noise analysis of neuronal light responses. *Network* 12:199–213.
- Flores-Herr N, Protti DA, Wässle H (2001) Synaptic currents generating the inhibitory surround of ganglion cells in the mammalian retina. *J Neurosci* 21:4852–4863.
- Cook PB, McReynolds JS (1998) Lateral inhibition in the inner retina is important for spatial tuning of ganglion cells. *Nat Neurosci* 1:714–719.
- Sinclair JR, Jacobs AL, Nirenberg S (2004) Selective ablation of a class of amacrine cells alters spatial processing in the retina. *J Neurosci* 24:1459–1467.
- Kirsch J (2006) Glycinergic transmission. *Cell Tissue Res* 326:535–540.
- Legendre P (2001) The glycinergic inhibitory synapse. *Cell Mol Life Sci* 58:760–793.
- Fischer F, et al. (2000) Reduced synaptic clustering of GABA and glycine receptors in the retina of the gephyrin null mutant mouse. *J Comp Neurol* 427:634–648.
- Kirsch J, Wolters I, Triller A, Betz H (1993) Gephyrin antisense oligonucleotides prevent glycine receptor clustering in spinal neurons. *Nature* 366:745–748.
- Poulopoulos A, et al. (2009) Neuroligin 2 drives postsynaptic assembly at perisomatic inhibitory synapses through gephyrin and collybistin. *Neuron* 63:628–642.
- Südhof TC (2008) Neuroligins and neurexins link synaptic function to cognitive disease. *Nature* 455:903–911.
- Craig AM, Kang Y (2007) Neurexin-neuroligin signaling in synapse development. *Curr Opin Neurobiol* 17:43–52.
- Jamain S, et al.; Paris Autism Research International Sibpair Study (2003) Mutations of the X-linked genes encoding neuroligins NLGN3 and NLGN4 are associated with autism. *Nat Genet* 34:27–29.
- Laumonier F, et al. (2004) X-linked mental retardation and autism are associated with a mutation in the NLGN4 gene, a member of the neuroligin family. *Am J Hum Genet* 74:552–557.
- Zhang C, et al. (2009) A neuroligin-4 missense mutation associated with autism impairs neuroligin-4 folding and endoplasmic reticulum export. *J Neurosci* 29:10843–10854.
- Göldenagel M, et al. (2001) Visual transmission deficits in mice with targeted disruption of the gap junction gene connexin36. *J Neurosci* 21:6036–6044.
- Wachtmeister L (1998) Oscillatory potentials in the retina: What do they reveal. *Prog Retin Eye Res* 17:485–521.
- Keck T, White JA (2009) Glycinergic inhibition in the hippocampus. *Rev Neurosci* 20:13–22.
- Rubenstein JL, Merzenich MM (2003) Model of autism: Increased ratio of excitation/inhibition in key neural systems. *Genes Brain Behav* 2:255–267.
- Ritvo ER, et al. (1988) Electroretinograms in autism: A pilot study of b-wave amplitudes. *Am J Psychiatry* 145:229–232.
- Simmons DR, et al. (2009) Vision in autism spectrum disorders. *Vision Res* 49:2705–2739.
- Fitzpatrick D, Lund JS, Schmechel DE, Towles AC (1987) Distribution of GABAergic neurons and axon terminals in the macaque striate cortex. *J Comp Neurol* 264:73–91.
- Montero VM, Zempel J (1986) The proportion and size of GABA-immunoreactive neurons in the magnocellular and parvocellular layers of the lateral geniculate nucleus of the rhesus monkey. *Exp Brain Res* 62:215–223.
- Irie M, et al. (1997) Binding of neuroligins to PSD-95. *Science* 277:1511–1515.
- Clements JD, Bekkers JM (1997) Detection of spontaneous synaptic events with an optimally scaled template. *Biophys J* 73:220–229.
- Prusky GT, Alam NM, Beekman S, Douglas RM (2004) Rapid quantification of adult and developing mouse spatial vision using a virtual optomotor system. *Invest Ophthalmol Vis Sci* 45:4611–4616.